J Solid State Electrochem (2012) 16:3261–3266
DOI 10.1007/s10008-012-1770-z

ORIGINAL PAPER

Electrochemical determination of isoprenaline using a graphene-modified glassy carbon electrode

Meifeng Chen · Xinying Ma · Xia Li

Received: 15 November 2011 / Revised: 28 April 2012 / Accepted: 2 May 2012 / Published online: 17 May 2012

Abstract The electrochemical determination of isoprenaline (IP) using a graphene-modified glassy carbon electrode (GME) was investigated by cyclic voltammetry. The results showed that the GME exhibited excellent electrochemical activity towards IP in pH 4.0 phosphate buffer solution (PBS). The reduction peak current (i_{pc}) of IP was linearly proportional to its concentration in the range of 2.1×10^{-7}–1.0×10^{-5} mol L^{-1} and 1.0×10^{-5}–1.0×10^{-4} mol L^{-1}, with the linear regression equations as $i_{pc1}(A) = -2.31 \times 10^{-6} + 6.96c$ (c/moles per liter), $R_1 = 0.9982$ and $i_{pc2} = 6.00 \times 10^{-5} - 0.49c$ (*c*/moles per liter), $R_2 = 0.9971$, respectively, and a detection limit of 6.4×10^{-8} mol L^{-1}. This method is of simplicity, rapidity, and high sensitivity and provides a practicable solution for the selective determination of IP in the presence of uric acid and ascorbic acid. The method has been successfully applied to IP sample analysis.

Keywords Isoprenaline · Graphene · Glass carbon · Electrochemistry

Introduction

Isoprenaline or isoproterenol (IP) is a sympathomimetic beta-receptor stimulant that has been used for the treatment of bradycardia (slow heart rate), heart block, etc. There are a number of side effects associated with the use of IP which may include heart palpitations, anxiety, fatigue, flushing, sweating, shaking, headache, and chest pain [1]. Therefore, it is essential to develop a simple and rapid method for its determination in routine analysis.

A variety of methods have been used for determining IP in tablets and biological fluids, for example fluorescence [2], spectrophotometric [3], nuclear magnetic resonance spectroscopy [4], and chemiluminescence [5, 6]. But these methods often suffer from the disadvantage of low sensitivity and/or complicated procedures. In recent years, electrochemical method has attracted wide attention due to its simplicity, fastness, sensitivity, and selectivity. Electrode modification, which has an important part in electrochemical studies, has been extensively used.

IP contains phenolic hydroxy groups and possesses electrochemical activity; therefore, various modified electrodes, for instance, copper(II) hexacyanoferrate(III)-modified electrode [7], ferrocene multiwall carbon nanotubes-modified electrode [8], and other modified electrodes [9–11], have been reported for the determination of IP. Electrodes modified with various nanomaterials have been used in electrochemical studies of some catecholamine compounds [12–17]. Due to the unique electronic and catalytic properties of these nanomaterials, these methods show good sensitivity, selectivity, stability, and low detection limits. Graphene, one of these nanomaterials, has attracted tremendous attention from both the theoretical and experimental scientific communities in recent years [18, 19]. It has been used to prepare a new generation of electrodes for electrochemical detection [13, 16, 20]. To the best of our knowledge, no literature has reported the determination of IP using graphene-modified electrodes.

In this paper, a novel electrochemical sensor was fabricated with graphene-modified glassy carbon electrodes. The electrochemical properties of the sensor were investigated. The results showed that the graphene-modified electrode (GME) exhibited excellent performance for detecting IP in the presence of uric acid (UA) and ascorbic acid (AA).

M. Chen (✉) · X. Ma · X. Li
Department of Chemistry and Chemical Engineering, Heze University,
Heze 274015, People's Republic of China
e-mail: chenmeifeng456@yahoo.com.cn

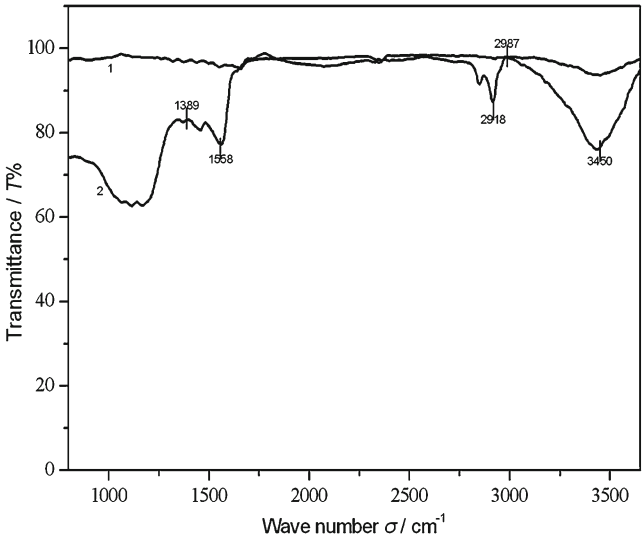

Fig. 1 IR of the graphite and graphene. *1* graphite; *2* graphene

Experimental

Reagents and apparatus

Graphite powder (<20 μm) was obtained from Qingdao graphite CO., LTD (Qingdao, China). Sodium borohydride was from Tianjin Daofu Chemical New Technique Development Co., LTD (Tianjin, China). Isoprenaline was purchased from Drug and Biological Products Examination Bureau of Beijing (Beijing, China). Injection forms of isoprenaline hydrochloride, uric acid, and ascorbic acid were purchased from Shanghai Harvest Pharmaceutical Co. Ltd, Shanghai (Shanghai, China). Phosphate buffer solutions were prepared by mixing the stock solution of 0.2 mol L^{-1} disodium hydrogen phosphate (Na_2HPO_4) and 0.1 mol L^{-1} citric acid ($C_6H_8O_7$). All other chemicals not mentioned here were analytical reagent grade. Double distilled water was used throughout. Graphene was made as described below.

Electrochemical experiments were performed with an Electrochemical Work Station-CHI660C (Chen-hua, Shanghai, China). Infrared spectra (IR) were recorded using a Varian 660-IR spectrometer (Agilent, America). Atomic force microscope (AFM) image was obtained using an Agilent 5500 AFM (Agilent, America). Scanning electron microscope (SEM) image was obtained using a field emission SEM Sirion 200 (FEI, America). Transmission electron microscope (TEM) image was obtained using a JEM-2010 transmission electron microscope (JEOL, Japan). Electrochemical experiments were carried out using a three-electrode system consisting of a working electrode (a bare or graphene-modified glassy carbon electrode, 3 mm in diameter), a counter electrode (a platinum wire electrode), and a reference electrode (a Ag/AgCl electrode). Acidity was measured by a PHS-3B Precision pH meter (Shanghai, China), and sonication was done using a KQ-100 Ultrasonic Cleaner (Kunshan, China).

Preparation of the nano-graphene

Graphene oxide (GO) was made by a modified Hummers method [21] using expandable graphite flake as starting material. Briefly, graphite flake (8 g) was stirred in 98 % sulfuric acid (180 mL) for 10 h. Potassium permanganate (24 g) was gradually added while keeping the temperature under 36 °C for 0.5 h. The mixture was then stirred at 80 °C for 45 min, and then water (360 mL) was added and the mixture heated at 95–105 °C for another 30 min. The reaction was terminated by addition of distilled water (360 mL) and 30 % hydrogen peroxide solution. The powder of GO was obtained by filtration.

A suspension [22] was obtained by dispersing GO in distilled water with the aid of intensive sonication. An

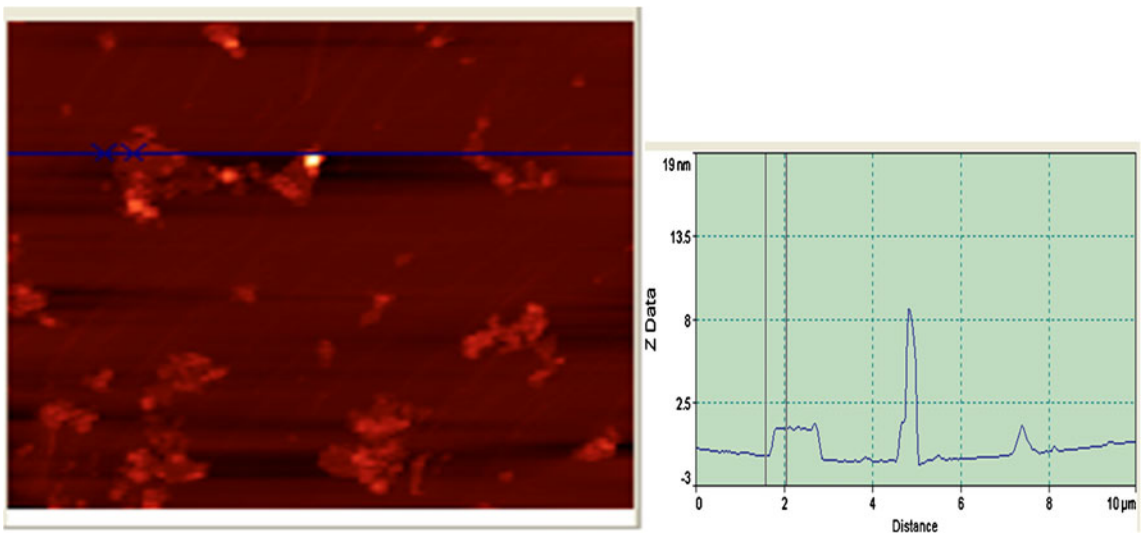

Fig. 2 AFM of the graphene

aqueous of pH = 10 GO suspension was prepared and then sodium borohydride was added. The temperature was strictly controlled by a constant temperature circulator at 80 °C for1.5 h. The powder of graphene was obtained by filtration and drying in vacuum and characterized by IR, AFM, TEM, and SEM.

Preparation of graphene-modified electrode

Graphene suspension (0.7 mg mL^{-1}) was prepared. Glassy carbon electrode (GCE) was polished before each experiment with gold sand paper and 0.05 μm alumina powder, respectively, then washed successively with 1:1 nitric acid, ethanol and doubly distilled water in ultrasonic bath, and dried in air. GME was prepared by casting 8 μL of graphene suspension at the GCE and dried under an infrared lamp.

Determination of IP

Under optimal conditions, a series of different concentrations of IP were investigated by cyclic voltammetry (CV) in phosphate buffer solution (PBS) solution (pH 4.0). A three-electrode system was used. CVs of IP were recorded. The GME was treated in PBS (pH 4.0) by repetitive scanning for 20 cycles in the potential range between 0 and 0.6 V at a scan rate of 140 mV s^{-1} so as to use again.

Results and discussion

Characterization of graphite/graphene/GME

Figure 1 shows the image of IR of graphite and graphene. The wave numbers of functional groups of C = C, C–O–C, and C–OH are 1,300–1,600, 1,110–1,200 (epoxide), and 3,450 cm^{-1}, respectively. These results show that the graphene has been synthesized successfully. The functionalized and defective graphene sheets are more hydrophilic and can be easily dispersed in solvents with long-term stability. Figures 2 and 3 show the AFM and TEM images of the graphene, respectively, revealing its mono- or few-layer sheet. Figure 4 shows the SEM image of the GME, revealing the crumple and wrinkle structure of the graphene film.

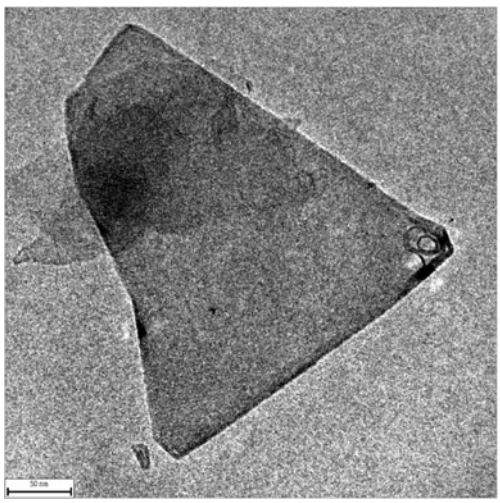

Fig. 3 TEM image of graphene

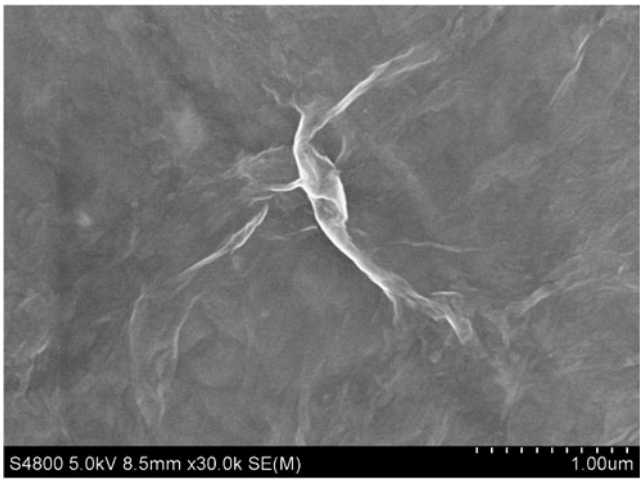

Fig. 4 SEM image of graphene film-modified GCE

Effect of concentration and amount of graphene

The amount of absorbed graphene on the GCE strongly affects the intensity of the peak current of IP. To find the optimal amount, the GME was prepared in different concentrations and amount of graphene suspension and used for the analysis of IP. The results showed that the peak current (I_p) increased with the increase of graphene concentration

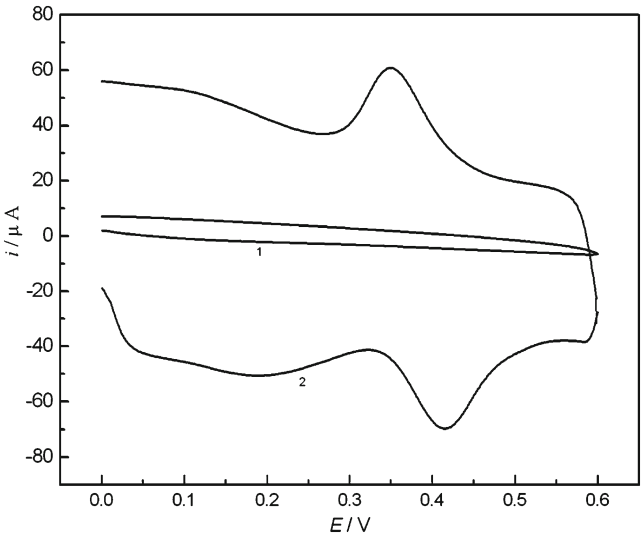

Fig. 5 CVs of IP (5.0×10^{-5} mol L^{-1}) at the GCE (*1*) and at the GME (*2*) in PBS (pH=4.0). Scan rate is 140 mV s^{-1}

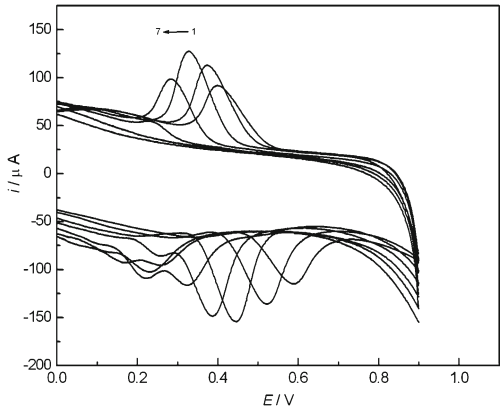

Fig. 6 CVs of 5.0×10^{-5} mol L^{-1} IP on the GME at scan rate of 140 mV s^{-1} in pH 4.0 PBS. The pH value of PBS: 1, 2.2; 2, 3.0; 3, 4.0; 4, 5.0; 5, 6.0; 6, 7.0; and 7, 8.0

from 0.3 to 0.7 mg mL^{-1}. The peak current decreased when the concentration of graphene exceeded 0.7 mg mL^{-1}, which may be ascribed to the thicker film of graphene hampering the electrical conductivity. Meanwhile, catalytic substrates are hampered when spreading to the electrode surface. In our experiments, 8 μL of 0.7 mg mL^{-1} suspension was used to modify the GCE.

Electrochemical behaviors of IP on the GME

The catalytic ability of the graphene towards the redox of IP was evaluated at the GCE and GME by CV. From Fig. 5, we can see that the peak currents of IP at the GME (2) were sharply increased in comparison with its response at the GCE (1), demonstrating the electrocatalytic activity towards IP. The electrocatalytic activity may be attributed to the unique physical and chemical properties of graphene. It also can be seen from Fig. 5 that E_{pa}=0.413 V, E_{pc}=0.350 V, i_{pa}=−28.77 μA, i_{pc}=37.71 μA, and i_{pa}/i_{pc} <1, suggesting that the reaction of IP at the GME is a quasi-reversible redox process. This electrochemical sensor showed excellent performance towards detecting IP.

Optimization of the experimental conditions

The effect of the medium's pH on the electrochemical signal was analyzed. Figure 6 shows the important influence of pH on the redox reaction of IP at the GME. As can be seen, the redox peak shifted negatively with increasing pH value of the solution. Based on [$E_p = (E_{pa} + E_{pc})/2$], the equation was

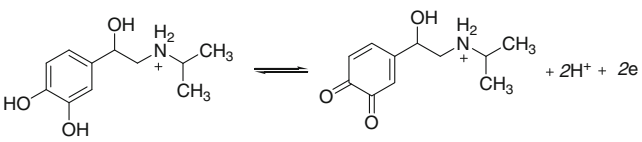

Scheme 1 Oxidation of IP

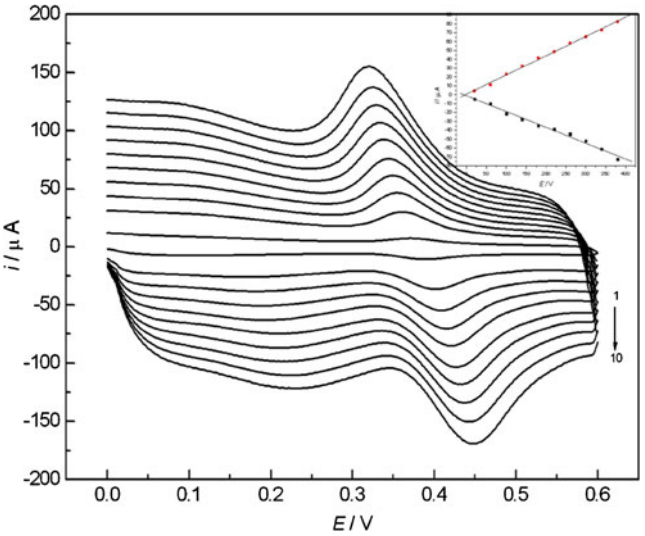

Fig. 7 CVs of 5×10^{-5} mol L^{-1} IP at the GME at different scan rates. Each of the numbers from 1 to 10 correspond to scan rates of 20, 60, 100, 140, 180, 220, 260, 300, 340, 380 mV s^{-1}, respectively

E_p=0.62–0.058pH, R=0.9989. According to the Nernst equation, the slope of −58 mV pH^{-1} reveals that the proportion of the electron and proton involved in the reactions is 1:1. As IP oxidation is a two-electron process, the number of protons involved is also predicted to be two. Therefore, a mechanism for the IP oxidation can be proposed in (Scheme 1) [23]. The redox peak currents increased as the pH changing from 2.2~4.0, then decreased after pH >4.0. So the buffer solution of pH 4.0 was chosen in this work.

Figure 7 shows that the redox peak currents increased and slightly shifted in the negative direction with the increase of scan rate from 20 to 380 mV s^{-1}. The redox peak currents

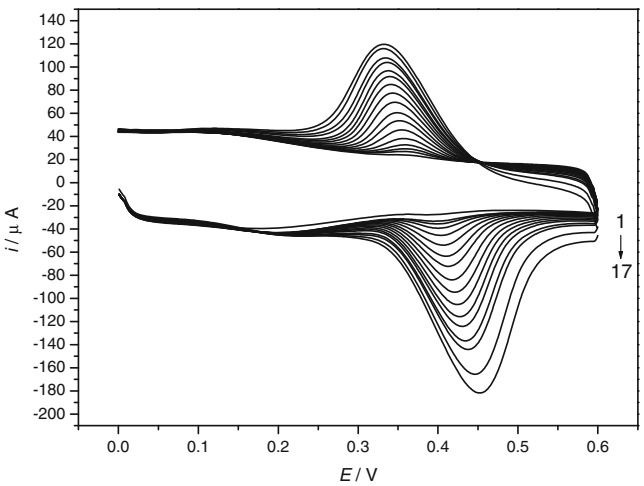

Fig. 8 CVs at the GME for different IP concentrations (1–17): 6.4×10^{-8}, 8.6×10^{-8}, 2.1×10^{-7}, 4.2×10^{-7}, 6.4×10^{-7}, 8.6×10^{-7}, 1.0×10^{-6}, 2.0×10^{-6}, 4.0×10^{-6}, 6.0×10^{-6}, 8.0×10^{-6}, 1.0×10^{-5}, 2.0×10^{-5}, 4.0×10^{-5}, 6.0×10^{-5}, 8.0×10^{-5} and 1.0×10^{-4} mol L^{-1}in PBS pH 4.0

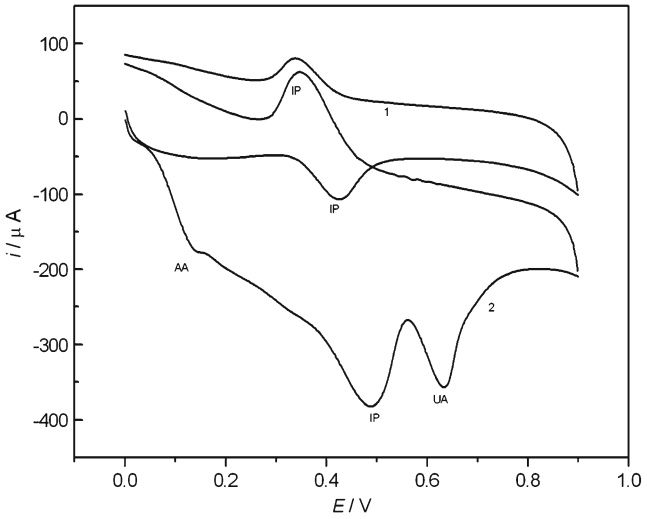

Fig. 9 CVs of *IP* (5.0×10^{-5} mol L^{-1}) (*1*) and *IP* (5.0×10^{-5} mol L^{-1}), *UA* (5.0×10^{-5} mol L^{-1}), and AA (1.0×10^{-3} mol L^{-1}) (*2*) on the GME in PBS (pH=4.0) with scan rate of 140 mV s^{-1}

linearly increased with the scan rates ranging from 20 to 380 mV s^{-1} (insert). The liner regression equations and correlation coefficients of the i_{pa} and i_{pc} of the scan rates are expressed as $i_{pa}=1.37 \times 10^{-6} + 2.14 \times 10^{-7}v$ (in millivolts per second), $R=0.9990$ and $i_{pc}=-4.20 \times 10^{-6} - 1.56 \times 10^{-7}v$ (millivolts per second), $R=0.9942$, respectively. It shows that the electrode process of IP at the GME is an adsorption process. If the GME was taken out from the solution of IP, we found that the redox peak currents still existed and decreased sharply with scanning time after time. It also may be ascribed to an adsorption process of electrochemical behaviors of IP on the GME. The peaks of IP were better at scan rate of 140 mV s^{-1} than other peaks. Therefore, 140 mV s^{-1} was used as the scan rate in our work.

Effect of accumulation time

The study of the variation of accumulation time enabled us to ascertain the level of IP adsorption on the GME. To accomplish this, we varied the accumulation time between 20 and 140 s for 5.0×10^{-5} mol L^{-1} IP and CVs of IP were recorded every 20 min. The peak currents increased as stirring time increased and reached a maximum at 100 s. Therefore, 100 s was used as the accumulation time.

Linearity range and detection limit

A series of different concentrations of IP in PBS (pH 4.0) were investigated by CV. The reduction peak current (i_{pc}) showed a linear relationship with its concentrations of IP over the range of 2.1×10^{-7}–1.0×10^{-5} mol L^{-1} and 1.0×10^{-5}–1.0×10^{-4} mol L^{-1} (Fig. 8). The linear regression equations with correlation coefficients were $i_{pc1}(A)=-2.31 \times 10^{-6} + 6.96c$ (in moles per liter), $R_1=0.9982$ and $i_{pc2}=6.00 \times 10^{-5} - 0.49c$ (in moles per liter), $R_2=0.9971$, with a detection limit of 6.4×10^{-8} mol L^{-1}.

Stability and reproducibility of the GME

The stability and reproducibility of the GME were studied by replicate determination of 5×10^{-5} mol L^{-1} IP. After each experiment, the GME was restored by a continuous scan in pH 4.0 PBS until no peak comes out. The six measurements achieved a good reproducibility with a relative standard deviation (RSD) of 4.5 %. A refreshed electrode surface could be used 20 times successively without obvious performance deterioration and the RSD was 5.3 %. The results indicated that the GME exhibited good reproducibility in the detection of IP.

Interference studies

As shown in Fig. 9, in order to confirm the availability of the GME to the selective determination of IP in the presence of UA and AA, we scanned the solution of 5.0×10^{-5} mol L^{-1} IP (curve 1) and a mixture containing 5.0×10^{-5} mol L^{-1} IP, 5.0×10^{-5} mol L^{-1} UA, and 1.0×10^{-3} mol L^{-1} AA (curve 2) in PBS (pH 4.0) by CV, respectively. IP has a pair of redox peaks but AA and UA have no reductive peaks at the GME from 0.0 to 0.9 V. So this method provides a practicable solution for the selective determination of IP in the presence of UA and AA in their mixture.

The effects of the other substances that often accompany IP in various pharmaceutical preparations were studied by CV. When the relative error is less than ±5 %, no interference was found when determination was performed in the presence of 1,000 μmol L^{-1} of K^+, Na^+, Ca^{2+}, NH_4^+, Mg^{2+}, Cl^-, SO_4^{2-}, PO_4^{3-}, β-alanine, and 100 μmol L^{-1} of glucose and tartaric acid.

Table 1 Determination of IP in injection

Sample	Amount of IP found in sample	Amount of standard IP added	Total amount of IP found	Recovery/%
1	6.08×10^{-5} mol L^{-1}	4.00×10^{-5} mol L^{-1}	10.05×10^{-5} mol L^{-1}	99.25
2	6.10×10^{-5} mol L^{-1}	4.00×10^{-5} mol L^{-1}	10.15×10^{-5} mol L^{-1}	101.2
3	6.05×10^{-5} mol L^{-1}	4.00×10^{-5} mol L^{-1}	10.03×10^{-5} mol L^{-1}	99.50

Analytical application

The proposed system was applied to the analysis of some commercial injections (2 mL:1 mg). Certain amounts of UA ($c_{UA}/c_{IP}=1$) and AA ($c_{AA}/c_{IP}=1{,}000$) were transferred into a 50-mL brown flask and diluted with PBS (pH 4.0). IP in the diluted solution was determined by CV at the GME and recoveries were calculated according to i_{pc}. They are in excellent agreement with the labeled values. The results are listed in Table 1.

Conclusions

The electrochemical determination of IP using a GME was investigated by CV. The GME exhibited excellent electrochemical activity towards IP in pH 4.0 PBS. The results demonstrated that graphene influenced the electron transfer of IP, UA, and AA. The proposed method can be applied for the detection of IP in pharmaceutical injection samples.

Acknowledgments This work was financially supported by the Shandong City High School Science and Technology Fund Planning Project of (J10LB64) and the Scientific Research Foundation of Heze University (XYJJKJ-4).

References

1. Chen X, Jin Y (2000) In: Chen X (ed) New pharmacology, 14th edn. People's Medical Publishing House, Beijing
2. Wang ZP, Zhang ZJ, Fu ZF, Fang LQ, Luo WF, Chen DL, Zhang X (2003) Anal Chim Acta 494:63–70
3. Solich P, Polydorou CK, Koupparis MA, Efstathiou CE (2000) J Pharm Biomed Anal 22(5):781–789
4. Talebpour Z, Haghgoo S, Shamsipur M (2004) Anal Chim Acta 506(1):97–104
5. Zhang C, Huang J, Zhang Z, Aizawa MS (1998) Anal Chim Acta 374:105–110
6. Huang J, Zhang C, Zhang Z (1999) Chin Chem Lett 9:843–847
7. Bonifácio VG, Marcolino LH Jr, Teixeira MFS, Fatibello-Filho O (2004) Microchem J 78(1):55–59
8. Ensafi AA, Khoddami E, Karimi-Maleh H (2011) Int J Electrochem Sci 6:2596–2608
9. Elrod L, Schmit JL, Morley JA (1996) J Chromatogr A 723:235–241
10. Kutluay A, Aslanoglu M (2010) Acta Chim Slov 57:157–162
11. Ensafi AA, Karimi-Maleh H (2010) Int J Electrochem Sci 5:1484–1495
12. Geim AK, Novoselov KS (2007) Nat Mater 6:183–191
13. Kang XH, Wang J, Wu H, Liu J, Aksay IA, Lin YH (2010) Talanta 81:753–759
14. Zhou M, Zhai Y, Dong S (2009) Anal Chem 81:5603–5613
15. Alwarappan S, Erdem A, Liu C, Li CZ (2009) J Phys Chem C 113:8853–8857
16. Li F, Chai J, Yang H, Han D, Niu L (2010) Talanta 81:1063–1068
17. Guo S, Wen D, Zhai Y, Dong S, Wang E (2010) ACS Nano 4:3959–3968
18. Novoselov KS, Geim AK, Morozov SV, Jiang D, Zhang Y, Dubonos SV, Grigorieva IV, Firsov AA (2004) Science 306:666–669
19. Zhang Y, Tan JW, Stormer HL, Kim P (2005) Nature 438:201–204
20. Kima YR, Bong S, Kang YJ, Yang Y, Mahajan RK, Kim JS, Kim H (2010) Biosens Bioelectron 25:2366–2369
21. Jr Hummers WS, Offeman RE (1958) J Am Chem Soc 80 (6):1339–1339
22. Si YC, Samulski ET (2008) Nano Lett 8(6):1679–1682
23. Blanco-López MC, Lobo-Castañón MJ, Miranda-Ordieres AJ, Tuñón-Blanco P (2007) Electroanalysis 19:207–213